PROBABILISTIC TSUNAMI HAZARD ASSESSMENT BASED ON THE GUTENBERG–RICHTER LAW IN MENTAWAI SUBDUCTION ZONE

Akbar Rian Setyahagi[1] **Supervisor :Toshitaka BABA**[2]

ABSTRACT

This study calculates tsunami hazards along the coastal area of the West Sumatra Regency using Probabilistic Tsunami Hazard Assessment (PTHA). A total of 22,714 earthquake scenarios were generated based on stochastic slip distributions correlated with the Gutenberg–Richter (G–R) law. Tsunami simulations were conducted using the JAGURS software with Message Passing Interface parallelization on the Earth Simulator supercomputer. The results show that the highest tsunami hazard occurred in the Mentawai Islands, particularly North Pagai Island, where tsunami heights reach 6.63 m for a 100-year return period, whereas mainland areas such as Padang and Padang Pariaman record much lower heights, generally below 2.5 m. This pattern is consistent for the 500- and 1000-year return periods, with tsunami heights on the islands exceeding 10 m, and those on the mainland remaining below 5 m. Sensitivity tests on G–R parameters, such as minimum magnitude, source depth, and standard deviation, showed a minimal impact on the hazard curve. In addition, comparison with the historical tsunami events of 1797 and 1833 reveals that the annual exceedance rate of historical tsunamis is consistent with the hazard curve at the 3-m threshold. Disaggregation analysis demonstrates that fault segment contributions are based on location, which is relatively consistent with the return periods. These findings support the reliability of the PTHA for tsunami risk-mitigation planning in coastal West Sumatra.

Keywords: Probabilistic Tsunami Hazard Assessment (PTHA), Annual Exceedance Rate (AER), Gutenberg–Richter (G–R) Law.

1. INTRODUCTION

Indonesia is a country with high seismic activity because it lies at the convergence of three major tectonic plates. One key region of interest is the Sunda Megathrust, an extensive subduction zone stretching around 5,500 kilometers, which is recognized as the most significant tectonic boundary in the country (Sieh, 2005). According to data from the NCEI/WDS Global Historical Tsunami Database (NOAA National Centers for Environmental Information, 2025), there have been at least 14 earthquakes in the Sunda Megathrust zone over the past 250 years that have produced tsunamis with wave heights exceeding 1 meter. One critical portion of the Sunda Megathrust for tsunami hazard analysis is the Mentawai segment, located off the west coast of Sumatra. This segment has historically generated several major tsunamigenic earthquakes, including those in 1797, 1833, 2007, and 2010. Based on the tsunami potential along this subduction zone, applying Probabilistic Tsunami Hazard Assessment (PTHA) is crucial to evaluating long-term tsunami risk, especially in vulnerable coastal areas.

2. DATA

Bathymetric data were obtained from the Geospatial Information Agency of Indonesia (BIG), with spatial data at 6 arc-second intervals. Earthquake catalog data from 1906 to 2022 were combined from the USGS and BMKG, and the Global Centroid Moment Tensor (GCMT) catalog from 1976 to 2022.

[1] Agency for Meteorology, Climatology, and Geophysics (BMKG), Indonesia.
[2] Professor, Graduate School for Social and Industrial Science and Technology, Tokushima University.

3. METHODOLOGY

3.1. Stochastic Slip Distribution

Moment magnitudes (Mw) ranging from 6.8 to 8.9 were adopted from the Indonesian Earthquake Study Center (Pusgen, 2024), covering three megathrust segments: Mentawai–Siberut, Pagai, and Batu. The method proposed by Murphy & Herrero (2020) was adopted to generate stochastic heterogeneous slip distributions based on non-planar fault geometries (k223d) with a 5 km fault grid, the rupture area derived from Strasser et al. (2010) for subduction interface events, and assuming rigidity of 30 GPa and setting a uniform probability density distribution to generate stochastic slip variability. Rmax = 0.4, representing the maximum sub-event radius relative to the fault width, and na = 5000, indicating the number of sub-events forming a single slip pattern. A total of 10 slip scenarios were generated for each magnitude, and the results are shown in Figure 1, which demonstrates the differences across various magnitudes.

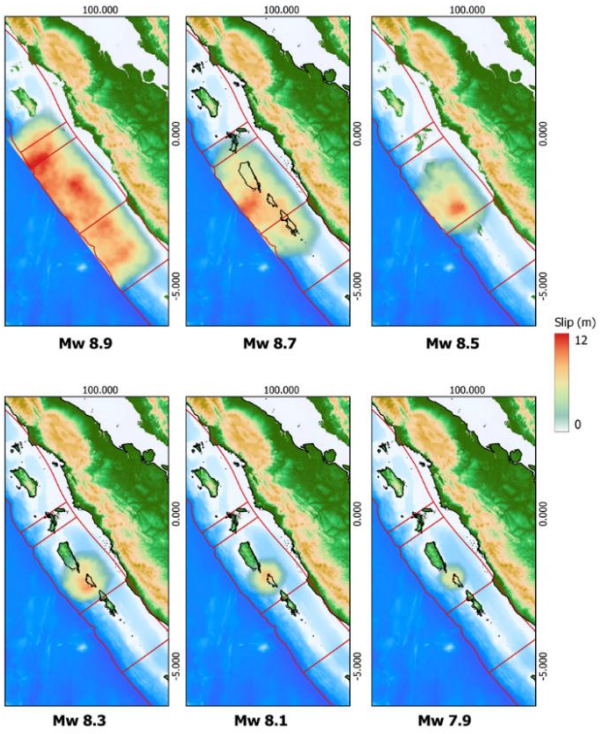

Figure 1. Examples of stochastic slip distribution generated using k223d for inputs Mw 8.9, 8.7, 8.5, 8.3, 8.1, and 7.9.

3.2. Constructed Fault Parameter

Gridded fault model with sub-fault dimensions of 20 km × 20 km was applied,with a total length and width of 627 x 229, as shown in Figure 2. Slip distribution output stochastic slip software k223d. The depth and dip angle of each fault were derived from the USGS Slab model (Hayes et al., 2018), with depths increasing from the trench toward the downdip end of the segment. The strike angle is assumed to be 323°, and a constant rake angle of 90° is applied to represent pure thrust faulting. Fault scenarios ranging from Mw 6.8 to 8.9 and were combined with 10 different stochastic slip realizations, leading to a total of 22,714 unique fault scenarios, which are summarized in Table 1.

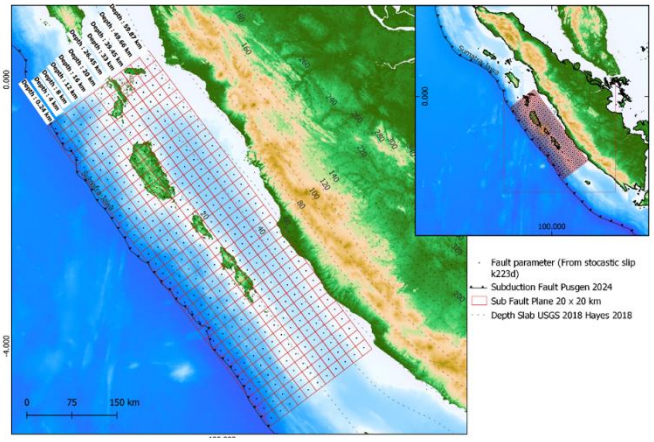

Figure 2. Sub fault location for this study. The point circles represent location slip faults from stochastic k223d s and depth, based on Hayes et al. (2018).

Table 1. Total number of scenarios for each magnitude.

Mw	Shifting	Stochastic	Mw	Shifting	Stochastic	Mw	Shifting	Stochastic
6.8	300	3,000	7.6	139	1,390	8.4	11	110
6.9	252	2,520	7.7	116	1,153	8.5	9	91
7	211	2,110	7.8	109	1,044	8.6	7	70

7.1	195	1,966	7.9	92	918	8.7	4	38
7.2	172	1,766	8	67	674	8.8	1	10
7.3	173	1,730	8.1	53	531	8.9	1	10
7.4	173	1,730	8.2	32	320	Total		22,714
7.5	140	1,413	8.3	12	120			

3.3. Tsunami Calculation

Tsunami simulations were performed using the open-source JAGURS code, executed in parallel computing MPI (Message Passing Interface) from the Earth Simulator supercomputer by the Japan Agency for Marine-Earth Science and Technology (JAMSTEC). The simulation code calculates displacements on the sea surface computation by Okada (1985) and solves nonlinear long-wave equations. A nested grid system consisted of two regions with a resolution of 54 and 18 arc seconds. Region 2 (18 arc-seconds) served as the base data used to determine the tsunami hazard evaluation points along the coastline. Tsunami simulations were run for 3 hours using a numerical time step of 0.5 s.

3.4. Earthquake occurrence probability based on the Gutenberg-Richter (G–R) law

Following the approach of Baba et al. (2022), we selected earthquakes with magnitude M > 5, focal depth < 50 km, and area only for Megathrust Batu, Mentawai-Siberut, and Mentawai–Pagai. We identified 68 out of 79 events indicatives of reverse or dip-slip faulting. We derived the equation by combining this with the earthquake catalog and normalizing over a 114-year data period.

$$\log_{10}(n\,M) = 4.88 - 0.86M \pm 0.014 \quad (1)$$

where nM is the annual rate of reverse-type seismic events of magnitude M. Sample scenarios were generated for each magnitude by using this relationship to estimate the resulting tsunami hazards.

3.5. Tsunami Hazard Analysis

Log-normal distribution was applied to represent the uncertainty in tsunami heights generated by each scenario. The following equation shows the probability that a tsunami will exceed a sure threshold height h assuming the model estimates of a maximum height H_{cal}.

$$P\,(H > h|H_{cal}) = 1 - \phi\left(\frac{ln\,h - ln\,H_{cal}}{\sigma}\right) \quad (2)$$

The parameter σ is introduced to reflect epistemic uncertainty in the tsunami modeling process and is explored over a range of values (e.g., 0.05, 0.20, 0.35, 0.50, 0.65, 0.80, 0.95) from smallest to largest spread. To compute the total annual exceedance rate of tsunami height h, we aggregated the contributions from
multiple earthquake scenarios using the following expression:

$$P(H > h) = 1 - \prod_{i=1}^{x}\{1 - P\,(E_i)P(H > h)|H_{cal})\} \quad (3)$$

where $P\,(E_i)$ is the annual occurrence rate of the i-th earthquake scenario, which is calculated from the G–R frequency magnitude distribution derived from the seismicity of the study area.

4. RESULTS AND DISCUSSION

4.1. Probabilistic Tsunami Hazard Result

Tsunami hazard maps illustrate the spatial distribution of maximum tsunami heights based on coastal point. Based on Figure 3, for the 100-year return period, the highest tsunami was 6.63 meters recorded in North Pagai, followed by Sibura, Tanahbala, South Pagai, and Siberut, with heights ranging from 3 to 4 meters. In contrast, the mainland coast of West Sumatra, including areas such as Padang and Padang Pariaman, shows much lower tsunami heights, generally below 2.5 meters. This trend continues in the 500- and 1000-year return periods, where tsunami heights in the Mentawai Islands exceed 10 meters, while they remain remains below 5 meters on the adjacent mainland.

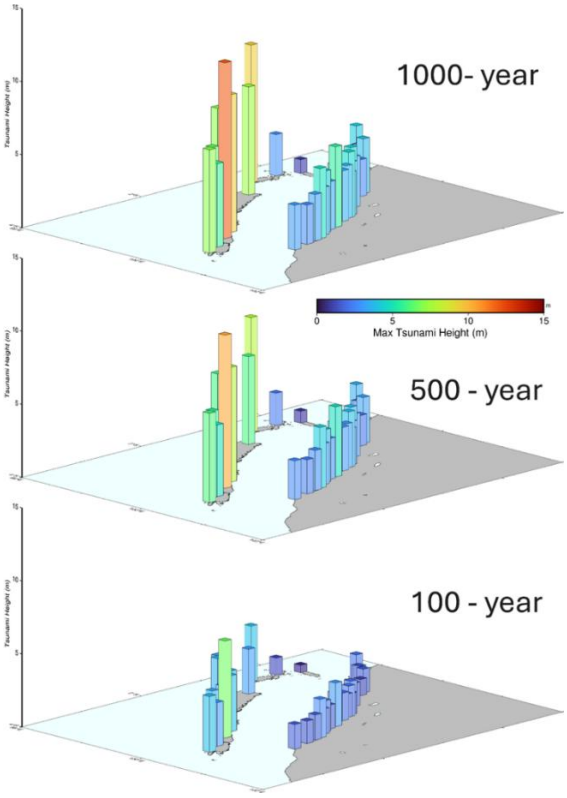

Figure 3. Tsunami hazard maps for 100-, 500-, and 1000- year return periods.

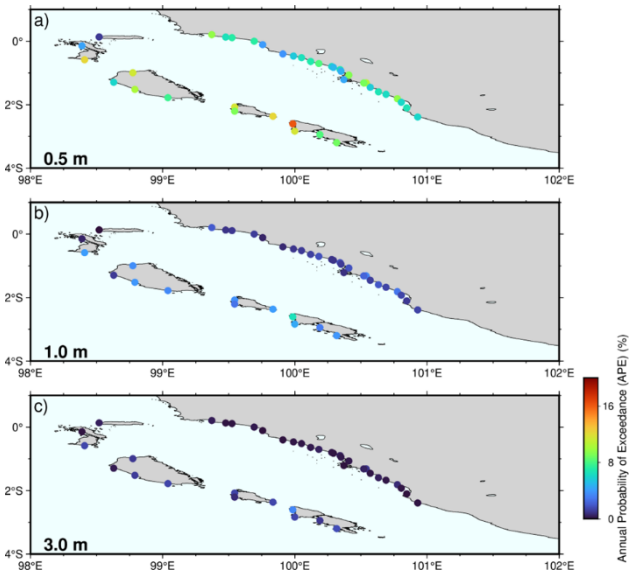

Figure 4. Annual probability of exceedance for 0.5, 1. and 3 m thresholds.

Figure 4 shows the annual probability of exceedance (as a percentage) for tsunami heights of 0.5 m, 1.5 m, and 3 m, along the coastline. Mentawai Islands show the highest annual probabilities for tsunami heights of 0.5 m, ranging from 10% to 16%, which is significantly higher than along the mainland West Sumatra coast, where values remain below 9%. A similar pattern was observed for the 1.5 m threshold, with Mentawai region showing probability between 3.2% and 6.5%, whereas those on the mainland coast remain under 2.5%. For the 3 m threshold, the highest annual probability is recorded at 3.4% in North Pagai, with most coastal points in the Mentawai Islands exceeding 1%, whereas the mainland coast of West Sumatra shows markedly lower values, generally below 0.5%.

4.2. Sensitivity Test Setting

The sensitivity setting of the G–R Law can assess the impact of variations in seismicity parameters. Several scenarios were tested, including changes in the slope (b-value), minimum magnitude threshold, earthquake source region, and faulting mechanism, as summarized in Table 2. Results shown in Cases B, C, D, E, and G, which involve adjustments to standard deviation, minimum magnitude threshold, event depth, or faulting mechanism, do not significantly impact on the tsunami hazard. Only Case F,

which uses the entire Sumatra Megathrust as the earthquake source, shows a clear increase in tsunami heights at an AER of 10,000-year return period.

Table2. G–R Law equations for sensitivity test.

	a	b	c	G–R Law based on
A	4.88	0.86	0	M > 5, Eq. catalog 1908 - 2022, Depth < 50 km, (Megathrust Batu, Mentawai Siberut, Mentawai Pagai) dip-slip reverse fault type
B	4.88	0.86	- 0.014	Same with A, reduced standard deviation
C	4.88	0.86	+ 0.014	Same with A, added standard deviation
D	4.87	0.86		M > 2, besides that the case same as A
E	4.89	0.85		all depths, besides that the case same as A
F	5.03	0.81		all segment Megathrust Sumatra, besides that the case same as A
G	4.94	0.86		All fault types, besides that the case same as A

4.3. Comparison with Historical Tsunamis

PTHA results were compared with two major historical tsunamis that struck Padang in 1797 and 1833 (Natawidjaja et al., 2006). These events are represented on the graph in Figure 5, showing their estimated annual exceedance rates (AER) based on historical records. The AER was calculated by dividing the number of events by the number of years since they occurred. For example, two tsunamis over 228 years yield a rate of 2/228, or approximately 8.77×10^{-3} per year. The results show that the AER of historical tsunamis is consistent with the hazard curve at the 3-meter threshold. Therefore, the PTHA we propose appears to be reasonably consistent with the limited historical tsunami data available.

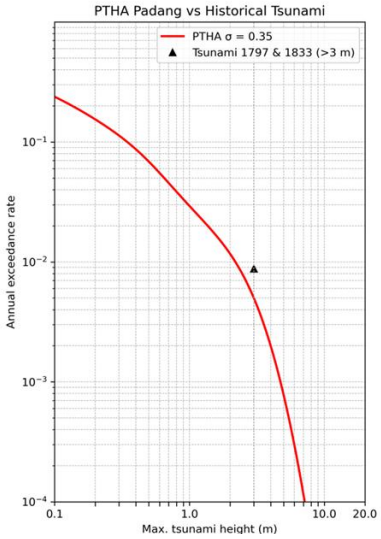

Figure 5. Tsunami Hazard curve and compare results with historical tsunami height.

4.4. Disaggregation Hazard Map

Tsunami hazard disaggregation identifies which parts of the megathrust fault contribute most significantly to tsunami potential at a specific location, based on the combination of earthquake magnitude and source-to-site distance (Kwong et al., 2015). In this study, we applied disaggregation analysis for Padang city, using a 100-year return period as the reference. The results show that at the Padang case point in Figure 6, tsunami with a maximum height of 2.19 meters is primarily caused by the Mentawai Siberut segment (54.22%), followed by the Batu segment (29.88%) and the Pagai segment (15.9%).

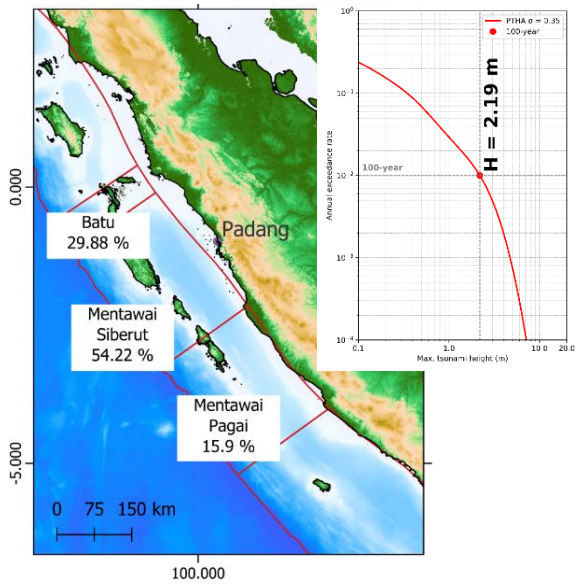

Figure 6. Disaggregation hazard map of each megathrust based on 100-year period.

5. CONCLUSIONS

Based on the tsunami hazard maps, the highest hazard area was located in the Mentawai Islands, with average tsunami heights of 3 – 6.63 meters for the 100-year return period. The mainland areas of West Sumatra, such as Padang and Padang Pariaman, show significantly lower tsunami heights, generally below 2.5 meters for the same return period. This pattern is consistent for the 500- and 1000-year return periods. Sensitivity tests for G–R parameters, such as standard deviation, minimum magnitude, source depth, and faulting mechanism, indicate that variations in these values do not significantly affect the overall shape of the tsunami hazard curves. Hazard curves were validated using historical tsunami events, such as those in 1797 and 1833. The results show that the AER of historical tsunamis is consistent with the hazard curve at the 3-m threshold. Disaggregation demonstrates that fault segment contributions vary by site, with relatively consistent patterns across the 500-year return period.

ACKNOWLEDGEMENTS

I would like to express my deepest gratitude to my supervisor, Prof. Toshitaka Baba from Tokushima University and my advisor Dr. Yushiro Fujii, who provided input and encouragement for this project. This study was supported by IISEE/BRI, JICA and GRIPS.

REFERENCES

Baba, T., Kamiya, M., Tanaka, N., Sumida, Y., Yamanaka, R., Watanabe, K., & Fujiwara, H. (2022). Probabilistic tsunami hazard assessment based on the Gutenberg–Richter law in eastern Shikoku, Nankai subduction zone, Japan. Earth, Planets and Space, 74(1), 156.

Hayes, G. P., Moore, G. L., Portner, D. E., Hearne, M., Flamme, H., Furtney, M., & Smoczyk, G. M. (2018). Slab2, a comprehensive subduction zone geometry model. Science, 362(6410), 58-61.

Kwong, N. S., Coppersmith, K. J., Bommer, J. J., & Abrahamson, N. A. (2015). Seismic hazard disaggregation: Past, present and future 12th International Conference on Applications of Statistics and Probability in Civil Engineering (ICASP12), Vancouver, Canada.

Murphy, S., & Herrero, A. (2020). Surface rupture in stochastic slip models. Geophysical Journal International, 221(2), 1081-1089.

Natawidjaja, D. H., Sieh, K., Chlieh, M., Galetzka, J., Suwargadi, B. W., Cheng, H.,…Ward, S. N. (2006). Source parameters of the great Sumatran megathrust earthquakes of 1797 and 1833 inferred from coral microatolls. Journal of Geophysical Research: Solid Earth, 111(B6).

NOAA National Centers for Environmental Information (2025, June, last access). National Geophysical Data Center / World Data Service: NCEI/WDS Global Historical Tsunami Database. https://doi.org/10.7289/V5PN93H7

Okada, Y. (1985). Surface deformation due to shear and tensile faults in a half-space. Bulletin of the seismological society of America, 75(4), 1135-1154.

Sieh, K. (2005). Aceh-Andaman earthquake: what happened and what's next? In *Nature* (Vol. 434, pp. 573-574). https://doi.org/10.1038/434573a

Strasser, F. O., Arango, M., & Bommer, J. J. (2010). Scaling of the source dimensions of interface and intraslab subduction-zone earthquakes with moment magnitude. Seismological Research Letters, 81(6), 941-950.

Pusgen (2024). Peta Sumber dan Bahaya Gempa Indonesia Tahun 2024. Pusat Penelitian dan Pengembangan Perumahan dan Permukiman, Kementerian PUPR.